Sains Malaysiana 51(4)(2022): 1261-1269
http://doi.org/10.17576/jsm-2022-5104-24

Solar Radio Burst Type II Characteristics and Coronal Mass Ejections (CMEs) Structure Based on the Presence of a Moreton Wave

(Pencirian Letupan Suria Radio Jenis II dan Struktur Letusan Jisim Korona (CME) Berdasarkan Kehadiran Gelombang Moreton)

Z.S. HAMIDI[1,2*], N.H.ZAINOL[2], N.N.M.SHARIFF[2,3] & N. MOHAMAD ANSOR[1,2]

[1]School of Physics and Material Science, Faculty of Applied Sciences, Universiti Teknologi MARA, 40450 Shah Alam, Selangor Darul Ehsan, Malaysia
[2]Institute of Science, Universiti Teknologi MARA, 40450 Shah Alam, Selangor Darul Ehsan, Malaysia
[3]Academy of Islamic and Contemporary Studies, Universiti Teknologi MARA, 40450 Shah Alam, Selangor Darul Ehsan, Malaysia

Received: 20 June 2021/Accepted: 19 August 2021

ABSTRACT

The Moreton wave has been extensively studied in explaining the relation between solar flare, Coronal Mass Ejections (CMEs) and Solar Radio Solar Burst Type II (SRBT II) phenomena. The purpose of this study was to determine whether Moreton waves have an impact on CME structure based on SRBT II parameters. The drift rate and structures of 28 SRBT II events selected from year 2014 to 2017 and observed by using ground-based Compound Low-cost Low Frequency Transportable Observatory (CALLISTO) spectrometer were determined. The CME data such as width angle and velocity were obtained from Large Angle Spectroscopy Coronagraph Observatory (LASCO) instrument, while solar flare class and its Active Region (AR) were attained from the Geostationary Operational Environmental Satellite (GOES). From the results, impulsive CME events have X, M and C class of solar flare in the presence of Moreton wave by using GONG data archive while gradual CME were associated with C or B class of solar flare. Impulsive CMEs have an angle of width more than 60° and velocity more than 500 km/s associated with both herringbone (HB) and harmonic structure of SRBT II. However, 30% of gradual CMEs which are associated with HB structure of SRBT II did not accompany by Moreton wave presence. Therefore, we can deduce that the impulsive CMEs are formed under the influence of Moreton wave and gradual CMEs emerged without the Moreton wave, based on the structure of SRBT II.

Keywords: Active Region; coronal mass ejections; Moreton wave; solar flare; solar radio solar burst type II

ABSTRAK

Gelombang Moreton telah dikaji secara meluas dalam menerangkan hubungan antara suar suria, Letusan Jisim Korona (CMEs) dan fenomenon Letupan Suria Radio Jenis II (SRBT II). Tujuan kajian ini adalah untuk menentukan sama ada gelombang Moreton mempunyai kesan ke atas struktur CME berdasarkan parameter SRBT II. Kadar hanyutan dan struktur 28 kejadian SRBT II yang dipilih dari tahun 2014 hingga 2017 dan diperhatikan dengan menggunakan peranti bumi spektrometer Majmuk Balai Cerap Boleh Angkut Kos Rendah Frekuensi Rendah (CALLISTO) telah ditentukan. Data CME seperti sudut lebar dan halaju diperoleh daripada instrumen Balai Cerap Graf Korona Spektroskopi Sudut Besar (LASCO), manakala kelas suar suria dan Wilayah Aktif (AR) diperoleh daripada Satelit Geopegun Operasi Alam Sekitar (GOES). Daripada keputusan, kejadian CME impulsif mempunyai kelas X, M dan C suar suria dengan kehadiran gelombang Moreton dengan menggunakan data arkib GONG manakala CME beransur-ansur dikaitkan dengan suar suria kelas C atau B. CME impulsif mempunyai sudut lebar lebih daripada 60° dan halaju lebih daripada 500 km/s yang dikaitkan dengan kedua-dua tulang ikan *herring* (HB) dan struktur harmoni SRBT II. Walau bagaimanapun, 30% daripada CME secara beransur-ansur yang dikaitkan dengan struktur HB SRBT II tidak disertai oleh kehadiran gelombang Moreton. Oleh itu, boleh disimpulkan bahawa CME impulsif terbentuk di bawah pengaruh gelombang Moreton dan CME beransur-ansur muncul tanpa gelombang Moreton, berdasarkan struktur SRBT II.

Kata kunci: Gelombang Moreton; letusan jisim korona; letupan suria radio jenis II; nyalaan suria; wilayah aktif

Introduction

The Moreton wave is another manifestation of flare induced Magnetohydrodynamic (MHD) shock wave in the corona (Wang et al. 2020). The Moreton wave is also known as a tsunami wave, a large-scale shock wave propagating in the chromosphere at average speed of Coronal Mass Ejection (CME) is more than 500 km s^{-1}. It is possible for a type II solar burst to appear along with Moreton waves in the metric range of wavelength (Cliver et al. 1999). It was first observed by Moreton (1960) and continued by Smith et al. (1971). The propagation of the phenomenon along the solar chromosphere surface takes place in a captive direction and even the small flare might produce one. The sweeping-skirt hypothesis by coronal MHD fast mode wavefront already explained by Uchida et al. (1973). The first Moreton waves correlated with solar burst type II has been found in the high corona (Kai 1969). In total, 13 events of Moreton waves have been recorded at Hα center, Hα±0.5 Å, and Hα±0.8 Å wavebands since 1997 (Zhang et al. 2011). A huge eruption of solar flare has been proposed as possible causes of coronal waves and shocks (Warmuth et al. 2004b). This is based on their speeds which can be comparable to typical Moreton wave speeds of 10^3 kilometers per second, as well as to the fact that they are often associated with coronal waves (Warmuth et al. 2004a). It was noted that the solar flares in Moreton events were characterized by an 'explosive phase' of sudden increase in brightness and a rapid expansion of the flare borders during the impulsive phase (Svestka 2012). The emission of the spikes by solar phenomena usually occurring in very short time and the small spatial scale is very significant to correlate the elementary processes of the magnetic field annihilation in the energy release region of the solar flare while the second fragmentation of the magnetic fields directly in radio source (Benz & Güdel 2010).

Meanwhile, Coronal Mass Ejection (CME) is a tremendous bubble full of magnetic field lines and plasma that was ejected from the solar source for a few minutes or hours that can be observed through coronagraph (solar disk) (Webb & Howard 2012). Generally, CME has an average speed of 450 km/s and within range of 100 km/s up to 3000 km/s (Zuccarello 2012). At early phase, typical CME carries mass of 10^{13} kg plasma material accelerates at the speed of several hundred km/s comes to the end when it reaches 2Rϵ, thus, the erupting magnetic material carries as a CME has an enormous amount of energy to be transmitted in a short time (Landi et al. 2010). At the end of 1995, a new spacecraft, Solar and Heliospheric Observatory (SOHO) was launched (Domingo et al. 1995) and instrument of Large Angle Spectrometry Coronagraph (LASCO) was upgraded to observe a CME event manually. However, this instrument has been upgraded from manual detection to an automated CME detection tool called Computer Aided CME Tracking Software (CACTUS) (Robbrecht & Berghmans 2004). The CMEs give impact to the Earth in the space weather condition by interrupting the Earth transmission system, power grid transmission and satellite communication system as well from the transmitted particle that carries high magnetic energy from the Sun (Howard 2014). This phenomenon will exchange its tremendous amount of energy with the magnetosphere of Earth when it spreads into the interplanetary space continue passing through the Earth's magnetosphere, thus, causing a geomagnetic storm to the Earth (Borovsky & Valdivia 2018).

Solar Radio Burst Type (SRBT) (I-V) indicated by different appearance on a dynamic spectrum. The SRBT II occurred because of the electrons accelerated in shocks while type III burst can be observed based on the accelerated electrons proliferating along open magnetic field lines (Lugaz et al. 2017). SRBT II occurs rarely during solar maximum and eventually become rarer to occur during a minimum phase of the solar cycle (Gopalswamy 2011). It is also called as metric type II bursts because they are typically observed at meter wavelengths. SRBT II can be divided into several types of class which were narrow bandwidth, harmonic structure, band splitting, multiple bands, compound type III-type II burst, Herring Bone (HB) structure and other fine structure. For instance, the main band structure of SRBT II has two sub-bands is because of the effect of magnetic splitting, analogous to the Zeeman Effect (Vršnak et al. 2002). Therefore, the slowly drifting feature in dynamic spectrum can be observed.

Among the types of SRBT II found, there were two most popular structures which are harmonic and HB structures (Cairns & Robinson 1987). As the burst drifting from high to low frequencies, at rate of typical type II burst, less than 1.0 MHz/s, the element of burst diverges from narrow band feature and appear on frequency time spectrogram as HB structure (Chernov 2011). There was a case where SRBT II formed a fundamental structure at the beginning of the mechanism within a few minutes' period but suddenly broken or split forming harmonic structure.

The SRBT II appearance due to CMEs components by Moreton wave as a driver is the subject to be

investigated further in this study. The aim of the study was to make a comprehensive analysis of the event associated and put forward the idea of Moreton wave and CMEs mechanism relation in association with SRBT II characteristics.

Methods

The methods of the research include two sections: (i) Moreton wave data of Hα filter from the (Global Oscillation Network Group (GONG) data archive, and (ii) CME data collection and analyzation from LASCO. The LASCO/SOHO satellite must be able to detect a propagating CME from the SRBT II data event selected. This data is available in Computer Aided CME Tracking (CACTus) website. We must ensure that all these CME events have high speeds or can be associated with a high solar flare event at the same time. Figure 1 shows an example of the image.

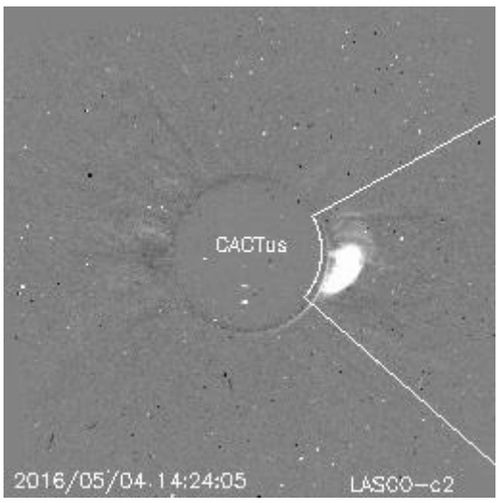

FIGURE 1. Coronagraph image of CME using CACTus LASCO/ SOHO in 4th May 2016

The data are correlated with solar radio burst type II either Herringbone or harmonic structure. Then, other event such as solar flare is identified with the idea that could trace Moreton wave presence near to the AR of solar flare. Both data events have obtained from GOES and GONG websites in collaboration with The National Aeronautics and Space Administration (NASA) which can be trusted and valid for the use of research. With these criteria, we found total 28 events that meet the criteria needed. The details events of solar activities and main parameters is presented in Table 1.

TABLE 1. Details events of solar activities and main parameters from 2014-2017

Event	Date	Flare event class (AR)	Moreton wave presence	Width angle of CME (°)	Type Herring Bone (HB)/ Harmonic(H)	Drift Rate (MHz/s)	Velocity of CME (km/s)
1	5/1/2014	No flare	No	50	HB	0.112	278
2	8/1/2014	M3.6(AR 11947)	Yes	108	H	0.393	367
3	25/01/2014	No data	Yes	80	H	0.534	299
4	26/01/2014	C1.5 (No data)	Yes	92	HB	0.419	1188
5	6/03/2014	No data	Yes	61	HB	0.464	520

6	20/04/2014	C6.4(AR 12033)	Yes	110	HB	0.099	347
7	27/05/2014	C4.9(AR 12065)	No	18	HB	0.089	389
8	23/06/2014	No flare	No	30	HB	0.079	190
9	22/08/2014	C2.2(AR 12146)	Yes	112	HB	0.228	372
10	24/08/2014	M5.9(AR 12151)	Yes	124	H	0.139	465
11	25/08/2014	M2.0(AR 12146)	Yes	125	H	0.076	520
12	23/09/2014	M2.3(AR 12172)	Yes	134	HB	0.190	331
13	28/09/2014	M5.1(AR 12173)	Yes	48	HB	0.394	215
14	2/10/2014	M7.3(AR 12173)	Yes	96	HB	0.013	367
15	22/10/2014	M1.4(AR 12197)	Yes	62	H	0.077	466
16	3/11/2014	M2.2(AR 12205)	Yes	121	H	0.355	228
17	11/03/2015	C1.7(AR12297)	Yes	74	H	0.210	240
18	12/04/2015	C2.9 (AR12320)	Yes	175	HB	0.117	678
19	28/08/2015	C4.5 (AR12403)	Yes	86	HB	0.049	370
20	16/10/2015	M1.1(AR12434)	Yes	83	H	0.271	189
21	9/11/2015	M3.9 (AR12450)	Yes	130	H	0.154	651
22	19/12/2015	C1.7(AR12469)	Yes	67	HB	0.167	767
23	16/03/2016	C2.2 (AR12522)	Yes	120	HB	0.072	529
24	2/05/2016	C3.5 (AR12540)	Yes	61	H	0.104	262
25	4/05/2016	C1.3 (AR12535)	Yes	70	H	0.058	383
26	07/09/2016	C5.2 (AR12573)	Yes	46	H	0.111	294
27	30/08/2017	B5.4 (No AR)	Yes	50	HB	0.065	245
28	06/09/2017	X9.3 (AR12673)	Yes	360	HB	0.145	978

Results and Discussion

In this section, the questions on how the Moreton wave gives effect to the CMEs characteristics based on the two structures categories of SRBT II (i) herring bone (HB); (ii) harmonic, are presented, specifically on the causes of the effects and the changes made. These questions can be answered by presenting selected well observed solar radio burst data, which shows a clear evolution or changes from Moreton waves to form SRBT II via CMEs phenomena. However, we would like to know the significance of these observations by determining the parameter which associated with the selected events. It is important to fully understand the process of CMEs by knowing the background environment especially in AR.

The total number of SRBT II occurred in four years from 2014 to 2017 is 28 events as listed in Table 1. The events were selected in 2014 because it is a year of solar maximum with the presence of highest number of SRBT II and the data selection is extended for three subsequent years to obtain larger data as well as to increase the results accuracy. Based on the analysis, the most frequent occurrence of SRBT II is in the year 2014 with 17 events, followed by 6 events in the year of 2015 while the least number of SRBT IIevent occurrence is in year 2016 and 2017 with 3 events, respectively. The pattern shows that the phenomena of SRBT II are decreasing gradually with selected year. The ending of solar maximum of Solar Cycle 24 began in 2014 as proven by the highest number of SRBT II, and it is followed by 2015 until 2017 which displayed a declination in SRBT II number. Thus, the activity of the Sun becomes weak as the Sun does not produce abundant magnetic energy. Moreover, during the minimum phase of Solar Cycle 24, fewer ARs are presented. Due to the lack of AR at one time, each event can be analyzed independently. Table 2 represents the total number of SRBT II within 3 years.

TABLE 2. Total number SRBT II in 2014 to 2017

No.	Year	Number of SRBT II
1	2014	16
2	2015	6
3	2016	3
4	2017	3
5	Total	29

Most of the SRBT II events have a HB structure with 18 case events and the number of the harmonic structure of SRBT II is only 11 events. This shows that the HB structure of SRBT II has been more frequent to occur. The frequency of occurrence for harmonic structure is almost consistent throughout the selected year compared to HB structure. Besides, the number of SRBT II HB structure occurrence has decreased from 2014 to 2017 compared to the harmonic structure. The number of SRBT II events for Herringbone and Harmonic structures is illustrates in Figure 2.

The disturbances produce in this regular band of SRBT II are the shock front of CME phenomena which accompanied by supersonic ejections. The structure is interpreted as the plasma radiation and generated by the electron stream accelerated at SRBT II shock. The ejections carry vast plasma of electrons, protons and other particles acts as the ejection disturbances produce the shock source elements of SRBT II. Besides, harmonic structure presents different configurations than HB structure. The intensities of fundamental and second harmonic band are different where the second harmonics

band has stronger intensities than fundamental due to insufficient non-linear plasma oscillation at an early stage of burst presence. It is also believed that some HB structure occurs in a condition where SRBT II is not associated with a CME due to the shock which is located away from the leading edge of the CME. Figure 3 shows the distribution of structure SRBT II from year 2014 to 2017 with associated drift rate.

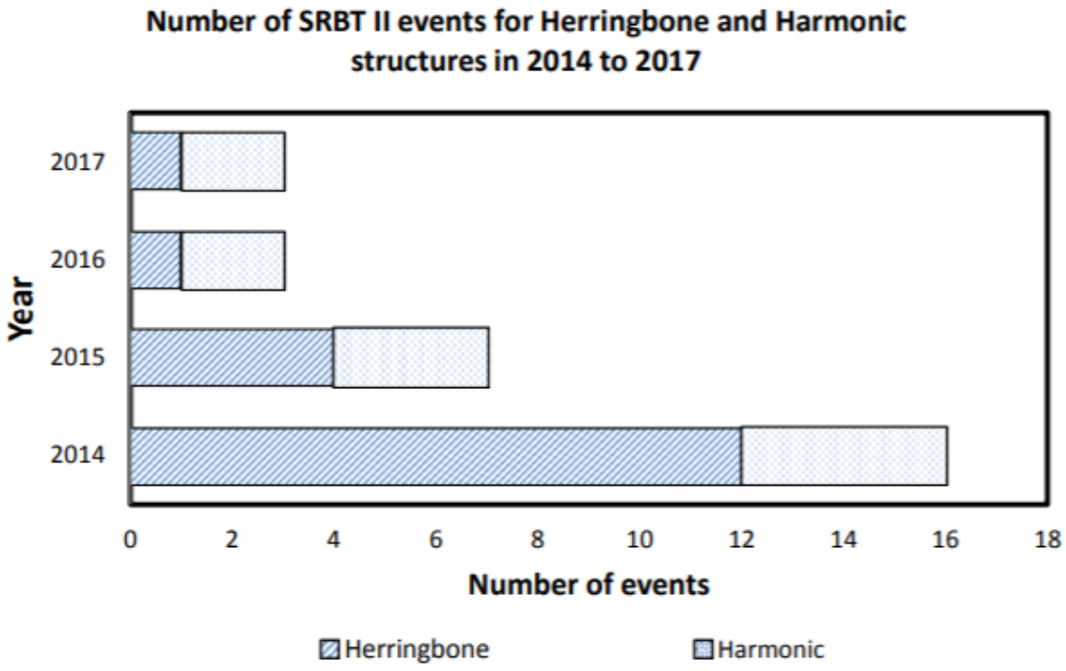

FIGURE 2. The classes of SRBT II based on its structure

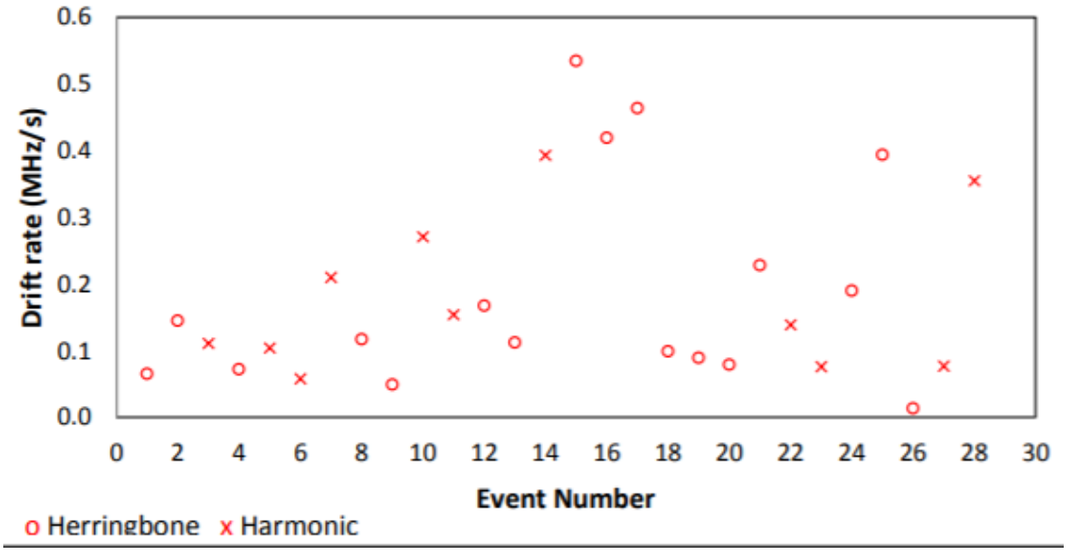

FIGURE 3. The distribution of structure SRBT II from year 2014 to 2017 with associated drift rate

However, there is a HB structure of SRBT II that drifted higher than 0.5 MHz/s reaches up to ~0.6 MHz/s. The difference in the drift rate for each SRBT II event depends on the mechanism, origin and surrounding SRBT IIcharacteristics which affects the propagation of SRBT II. Next, the focus will be on an analysis based on the temporal coincidence of the CMEs velocity and frequency drift rates of SRBT II, respectively. The SRBT II HB structure has a single band of area on the spectrogram interpreted as the signature of the radio burst formation. The drift rate is based on CALLISTO data while CMEs velocity is taken from the LASCO. Detailed results can be interpreted from Figure 4.

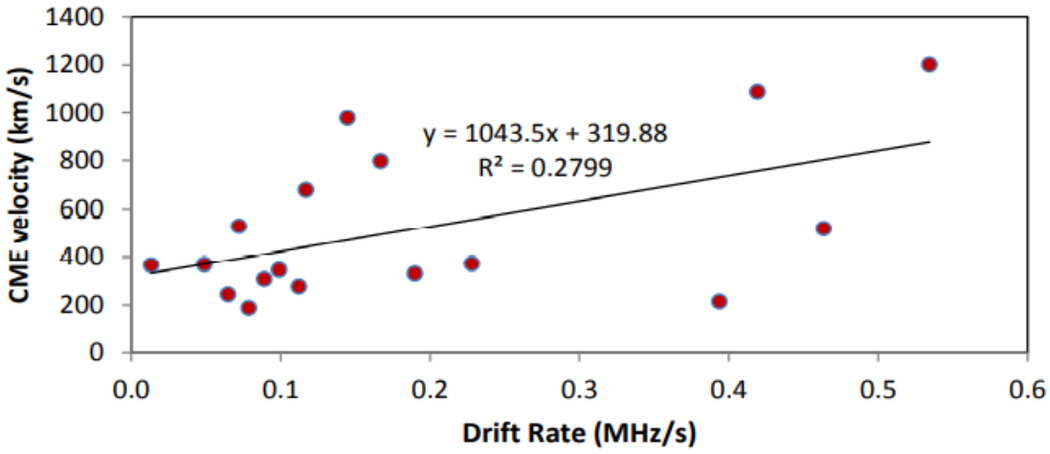

FIGURE 4. Drift rate of SRBT II against velocity of associated CME for Herring Bones (HB) structure cases

Although the distribution of the results might be dynamic, the CME velocity and SRBT II (HB structure) obtain a positive correlation, indicated by the linear increment of SRBT II drift rate and CME velocity in Figure 4. This data is based on data from 2014 through 2017. During this period of 4 years, the solar cycle is decreasing. According to the number of high solar flare events in 2014, there has been 38 M class and above solar events, compared to only 11 high solar flare events in 2017. Different solar activities and phases produce different levels of dynamic activity on the Sun, which affects CME velocity. The drift rate of plasma during SRBT II occurrence has a weak linear relationship to the velocity of CME where $R^2 = 0.2799$. Sun has dynamic activity occurs differently in each solar activity. Sun has dynamic activity occurs differently in each solar activity. Thus, one cannot confirm the activity of the Sun must follow the strong linear relationship perfectly. However, with numerous event numbers, the pattern can be estimated to be linear, but it is weak relationship. The gradient of the graph is 1043.5 km/MHz where it is quite distant ejection of plasma to the outer corona and IP medium. At zero drift rates, the CME velocity is estimated to drift at velocity 319.88 km/s where it is the initial velocity at onset of CME ejection.

The harmonic structure of SRBT II has the negative correlation as seen in Figure 5. As the drifting rate of SRBT II is increased, the velocity of CME decreases from 650 km/s to 180 km/s. This is because the plasma particles that releases during the harmonic SRBT II have loses its energy after CME phenomena. The slow drift rate of SRBT II harmonic structure causes the shifting and splitting band of SRBT II into several bands from abundant plasma erupted from the high velocity CME phenomena. The correlation has $R^2 = 0.1817$ which shows a weak linearity between the velocity of CME and the drift rate of harmonic SRBT II. However, the onset velocity of harmonic at zero drift rates is 463.21 km/s. This shows that the harmonic structure of SRBT IIhas a slower onset velocity compared to HB structure.

The high distribution both SRBT II HB and harmonic structure events in the slow drift rate range between 0.1-0.2 MHz/s has shown that the velocity of CME may reach up near 1000 km/s. HB structure has

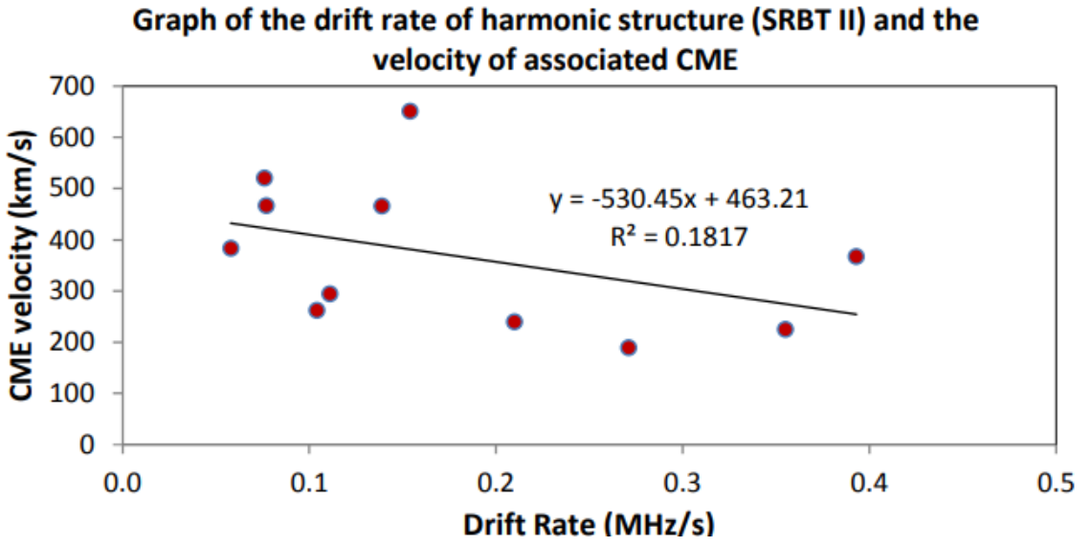

FIGURE 5. Drift rate of SRBT II against velocity of associated CME for Harmonic structure cases

positive distribution correlation because when the drift rate of SRBT II is increased then it causes the velocity of CME associated increases as well. However, the harmonic structure has reverse distribution correlation because even though the drift rate of SRBT II is increased, the velocity of associated CME decreases. Majority SRBT II events have a slow drift rate, which is approximately less than 0.2 MHz/s. This is due to typical SRBT II, which drifted slowly towards low frequency as it carries a large number of masses causing it to be heavy when it propagates out to the interplanetary and radiates its wavelength. The HB structure of SRBT IIhas a slow CME onset velocity compared to harmonic structure. This is due to insufficient non-linear plasma oscillation occurs in the corona. SRBT II harmonic structure has gradient smaller than SRBT II HB structure. The small gradient shown in the graph represents the less amount of energy being released during the ejection process due to the energy used for splitting the band into fundamental and harmonics band.

Previous studies have shown that Moreton waves are Coronal phenomena associated with type II bursts. We found that Moreton waves have a significant contribution to type II solar bursts with HB structures. An analysis of the width angle of CMEs has also been conducted in the presence of the Moreton wave. Those events in the presence of Moreton waves usually produce CMEs with the angular width of 60° and above, producing large CME bubbles accompanied by high-class (X, M, C) solar flares. There is no sign of the solar flare, causing Moreton wave absence. Consequently, the cases might be related to filament eruptions that can also cause CME phenomena. In addition, the results show that in the absence of a Moreton wave, the CME produces have a small angle of less than 60° in width. A weak solar flare presence or the absence of a Moreton wave can also be reasons for the lack of a Moreton wave. The absence of the solar flare also means there is no Moreton wave, but the CME phenomenon was triggered by the filament eruption.

Conclusion

The width angle of CME, solar flare class event along with the presence of Moreton wave has been discussed in detailed. There are 24 events were accompanied by Moreton wave presence among 28 events data. However, four events are not accompanied by Moreton wave presence due to no sign of the solar flare existence, causing Moreton wave absence. Nevertheless, 30% of gradual CME which associated with HB structure of SRBT II does not accompanied by Moreton wave presence. This indicates that Moreton wave presence causes enormous structure of CME bubble with angle

more than 60° width and velocity of above 500 km/s and often accompanied by harmonic structure of SRBT II. Thus, the cases might be related to filament eruption which also can produce the CME phenomena.

ACKNOWLEDGEMENTS

Special thanks go to SDO/AIA, NOAA, SWPC, LASCO, Helioviewer, Solar Monitor and Space Weather Live and E-CALLISTO websites for providing their data accessible to the public. Authors also give full appreciation to the reviewers and editors for the beneficial comments and suggestions. This work was partially supported by the grant, Young Talent Research Grant, 600-RMC/YTR/5/3 (001/2020) and the Ministry of Higher Education, Malaysia.

REFERENCES

Benz, A.O. & Güdel, M. 2010. Physical processes in magnetically driven flares on the sun, stars, and young stellar objects. *Annual Review of Astronomy and Astrophysics* 48: 241-287.

Borovsky, J.E. & Valdivia, J.A. 2018. The Earth's magnetosphere: A systems science overview and assessment. *Surveys in Geophysics* 39(5): 817-859.

Cairns, I.H. & Robinson, R.D. 1987. Herringbone bursts associated with type II solar radio emission. *Solar Physics* 111(2): 365-383.

Chernov, G.P. 2011. *Fine Structure of Solar Radio Bursts*. New York: Springer Science+Business Media. pp. 1-270.

Cliver, E.W., Webb, D.F. & Howard, R.A. 1999. On the origin of solar metric type II bursts. *Solar Physics* 187(1): 89-114.

Domingo, V., Fleck, B. & Poland, A.I. 1995. The SOHO mission: An overview. *Solar Physics* 162(1): 1-37.

Gopalswamy, N. 2011. Coronal mass ejections and solar radio emissions. *Planetary Radio Emissions* 7: 325-342.

Howard, T. 2014. *Space Weather and Coronal Mass Ejections.* New York: Springer Science+Business Media. pp. 1-96.

Kai, K. 1969. Radio evidence of directive shock-wave propagation in the solar corona. *Solar Physics* 10(2): 460-464.

Landi, E., Raymond, J.C., Miralles, M.P. & Hara, H. 2010. Physical conditions in a coronal mass ejection from Hinode, Stereo, and SOHO observations. *The Astrophysical Journal* 711(1): 75-98.

Lugaz, N., Temmer, M., Wang, Y. & Farrugia, C.J. 2017. The interaction of successive coronal mass ejections: A review. *Solar Physics* 292(4): 64.

Moreton, G.E. 1960. Hα observations of flare-initiated disturbances with velocities ~1000 Km/sec. *Astronomical Journal* 65: 494.

Robbrecht, E. & Berghmans, D. 2004. Automated recognition of coronal mass ejections (CMEs) in near-real-time data. *Astronomy & Astrophysics* 425(3): 1097-1106.

Smith, S.F., Harvey, K.L. & Macris, C.J. 1971. Physics of the solar corona. In *Proceedings of the NATO Advanced Study Institute, Astrophysics and Space Science Library* 27: 156.

Svestka, Z. 2012. *Solar Flares* (Vol. 8). Dordrecht, Holland: D. Reidel Publishing Company. pp. 1-349.

Uchida, Y., Altschuler, M.D. & Newkirk, G. 1973. Flare-produced coronal MHD-fast-mode wavefronts and Moreton's wave phenomenon. *Solar Physics* 28(2): 495-516.

Vršnak, B., Magdalenić, J., Aurass, H. & Mann, G. 2002. Band-splitting of coronal and interplanetary type II bursts-II. Coronal magnetic field and Alfvén velocity. *Astronomy & Astrophysics* 396(2): 673-682.

Wang, J., Yan, X., Kong, D., Xue, Z., Yang, L. & Li, Q. 2020. A small-scale filament eruption inducing a Moreton wave, an EUV wave, and a coronal mass ejection. *The Astrophysical Journal* 894(1): 30.

Warmuth, A., Vršnak, B., Magdalenić, J., Hanslmeier, A. & Otruba, W. 2004a. A multiwavelength study of solar flare waves-I. Observations and basic properties. *Astronomy & Astrophysics* 418(3): 1101-1115.

Warmuth, A., Vršnak, B., Magdalenić, J., Hanslmeier, A. & Otruba, W. 2004b. A Multiwavelength study of solar flare waves-II. Perturbation characteristics and physical interpretation. *Astronomy & Astrophysics* 418(3): 1117-1129.

Webb, D.F. & Howard, T.A. 2012. Coronal mass ejections: Observations. *Living Reviews in Solar Physics* 9(1): 1-83.

Zhang, Y., Kitai, R., Narukage, N., Matsumoto, T., Ueno, S., Shibata, K. & Wang, J. 2011. Propagation of Moreton waves. *Publications of the Astronomical Society of Japan* 63(3): 685-696.

Zuccarello, F. 2012. Data analysis and mathematical modeling of the initiation of coronal mass ejections. University of Leuven. Ph.D. Thesis (Unpublished).

*Corresponding author; email: zetysh@uitm.edu.my